Energy & Environmental Science

ADVANCED FUELS FROM ETHANOL-A SUPERSTRUCTURE BASED OPTIMIZATION APPROACH

Journal:	*Energy & Environmental Science*
Manuscript ID	EE-ART-07-2020-002447.R1
Article Type:	Paper
Date Submitted by the Author:	02-Dec-2020
Complete List of Authors:	Restrepo Florez, Juan Manuel; University of Wisconsin-Madison, Chemical and biological engineering Maravelias, Christos; Princeton University, Chemical and Biological Engineering; Andlinger Center For Energy And the Environment

ARTICLE

Advanced fuels from ethanol-A superstructure optimization approach

Received xx xxx xx,
Accepted xx xxx xx

DOI: 10.1039/x0xx00000x

Juan-Manuel Restrepo-Flórez[a], Christos T. Maravelias*[b]

We develop a superstructure framework for the design of biorefineries for ethanol upgrading into advanced biofuels to replace gasoline, jet fuel or diesel. The framework integrates catalysis, process synthesis, and fuel property modelling towards the design of biorefineries producing fuels with specified properties. The proposed framework is applied to idenitfy strategies for the upgrading of ethanol into one or more fuels with specific properties. We discuss the trade-off between profit and biorfinery complexity; as well as the relation among fuel property constraints, the optimal upgrading strategy selected, and process economics. Finally, we show how to find the optimal biorefinery associated with a particular chemistry or catalyst. The results presented constitute the first systematic study of ethanol upgrading considering, simultaneously, fuel and process design.

Broader context

Ethanol is the most common biofuel, typically blended with gasoline at a maximum 10% level. Considering current trends in fuel consumption and the expected increase in ethanol production capacity, it is projected that a surplus of ethanol will be available in the market. Consequently, numerous ethanol upgrading strategies have been studied. These strategies involve the use of several chemistries (e.g. dehydration, condensation, and Guerbet coupling) for the conversion of ethanol into different fungible molecules (e.g. olefins, alcohols, and ethers). However, the systematic analysis of these strategies is challenging due to the large number of available chemistries, catalysts, and processes. At the same time, there is a wide range of advanced biofuel targets, potentially outperforming their fossil-fuel-derived counterparts, whose properties could be tailored depending on the selected upgrading strategy. Accordingly, the goal of this work is to develop a framework for the design of novel and efficient ethanol upgrading strategies towards fuels with desirable properties. The interdisciplinary nature of the problem requires the integration of catalysis, process systems engineering, and fuel property modelling. We apply the proposed framework to design ethanol upgrading biorefineries that produce advanced biofuels designed to replace gasoline, jet fuel, or diesel.

Introduction

Concerns about global warming and energy independence have driven both governments and the private sector to invest in biofuel production research. The development of the ethanol industry is a notable example. Only in the U.S., ethanol annual production capacity has increased from 2 to 16 billion gallons in the last twenty years[1]. While the adoption of a biofuel is a significant development, ethanol has two important limitations. First, to prevent corrosion, regulations in most countries limit the amount of ethanol that can be blended with fuels to 10%[2,3]. Second, the demand for gasoline is decreasing[4,5] while the demand for middle distillates (diesel and jet fuels) is increasing[6], but ethanol is a poor replacement for middle distillates[5]. With the ethanol demand for gasoline blending satisfied[2], the increasing production capacity is likely to lead to a surplus of ethanol[1,7,8]. Accordingly, we have seen a renewed interest in finding strategies to upgrade ethanol into more fungible molecules[5,9,10]. Among these strategies, those leading to products that can be blended above 10% with fossil fuels are particularly important, especially if they can replace middle distillates.

In the last 30 years, the upgrading of ethanol toward fungible molecules has significantly advanced. The corpus of this literature covers a diverse set of chemistries (*e.g.* Guerbet coupling, dehydration, and condensation) and catalysts, establishing ethanol as a platform chemical[5,9,18,19,10–17]. Initial attempts to find ethanol upgrading strategies were oriented toward processes yielding final products similar to the ones derived from fossil fuels[5,10,18,20,21]. However, trying to develop biofuels with the same composition and properties as the ones derived from oil may be short-sighted. The diversity of ethanol chemistries can be used to design tailored fuels whose performance is as good as or even better than that of fossil fuels in an economically viable manner. However, there are important challenges in achieving this vision. First, the design space of the problem at hand is very large. Second it is necessary to consider the interactions among three areas: *catalysis*, *process synthesis,* and *fuel property modeling*.

While ethanol chemistries have been extensively reviewed[5,10], a comprehensive and systematic analysis of ethanol upgrading strategies has not been attempted. Towards this goal, an optimization-based process synthesis and analysis framework can be beneficial. Such a framework allows the exploration of a large design space, enables the identification of critical trade-offs, and leads to preliminary process designs that can be further explored using rigorous simulation tools. Although the application of optimization-based process synthesis is not yet the standard in industry, it has been successfully applied in academia to address both general synthesis problems (e.g. design of heat exchanger networks[22,23],

[a] Department of Chemical and Biological Engineering, University of Wisconsin–Madison, 1415 Engineering Drive, Madison, WI 53706, USA
[b] Department of Chemical and Biological Engineering, Princeton University, 50-70 Olden St, Princeton, NJ 08540, USA,
[c] Andlinger Center For Energy and the Environment, 86 Olden St, Princeton, NJ 08540 E-mail: maravelias@princeton.edu

†Electronic Supplementary Information (ESI) available. See DOI: 10.1039/x0xx00000x

distillation sequences[24,25], and integrated process flowsheets[26–29]), as well as specific systems (e.g. selection of biopolymer synthesis straegies[30], synthesis of biorefineries[2,31–34], and design of shale gas plants[35]). Of particular importance here are approaches dealing with the synthesis of integrated biorefineries. That is, biorefineries in which multiple technologies are employed[36–40]. Works in this field include efforts dealing exclusively with the process synthesis problem, without considering product properties[31,36,48,37,41–47], and to a lesser extent with the integrated process and product design problem[49–54]. The product design component has been viewed from two different perspectives. First, there are studies in which product design is understood as molecular design, that is, the product is a single chemical species with specified properties. This kind of formulation heavily relies on group contribution methods, and Quantitative Structure–Activity Relationships (QSAR)[50,53–57]. Alternatively, product design is formulated as a blend design, that is, the goal is to choose an optimal set of molecules, from an available candidate pool, such that the resulting blend has tailored properties, calculated using blending rules[39,49,51,58].

The integration of *catalysis*, *process synthesis*, and *fuel property modeling,* towards the formulation of a mathematical programming model can be achieved at two different levels: first, early-stage evaluation of candidate pathways; and second, evaluation of candidate flowsheets for which process information is available. In the early-stage evaluation, process information is limited. The goal is to find the optimal strategy, without performing detailed process simulations, using reasonable estimates of the total production costs, and the stoichiometry of a reaction network of interest[49,51,52,54]. Toward this direction, significant work has been carried out at the Fuel Design Center at RWTH Aachen University, where Reaction Network Flux Analysis (RNFA)[49,51,54,59] and Process Network Flux Analysis (PNFA)[51,60] were developed as support tools for the design of tailor-made biofuels. Along the same lines, Daoutidis and coworkers[52,61,62] studied the selection of an optimal pathway to obtain a product with specified properties. Other works of interest include those by Broadbelt and Shanks focused on the identification of bioprivileged molecules that can be easily transformed into other valuable chemicals[63–65]. A different problem arises when there exists detailed information (*i.e.* process flow diagrams and economic parameters) for several processes that can be used to produce a set of biofuels, either in a standalone manner or integrated into a more complex flowsheet. An interesting question concerns the identification of the network of processes that maximizes the profit while producing fuels with desired properties. In general, strategies to address this question have relied on superstructure-based optimization[31,36,37,39,45,46,48,66]. Notable examples include the Chemical Species/Conversion Operator (CSCO)[36] approach, the Biomass Utilization Superstructure (BUS)[31,45], the biomass bipartite graph representation (BBR)[43], the integer-cuts constraint method for biorefinery design[46,66], and the Processing Step-Interval Network (PSIN) representation[48,67]. However, most of these approaches do not consider the modeling of fuel properties, with the exception of the two-stage optimization approach by Ng and coworkers[39].

In this paper, we present a superstructure-based optimization framework that can be used for simultaneous process and fuel design, and we apply it to study ethanol upgrading to various biofuels. The results constitute the first systematic analysis of ethanol upgrading strategies, providing insights into conversion pathways, as well as identifying the major cost drivers associated with these strategies. Furthermore, we explore the trade-off between biorefinery complexity and process economics; and discuss the relation between the fuel properties and the optimal biorefineries designed. Methodologically, we express the problem using a hierarchical superstructure which encompasses detailed decisions (*e.g.* catalyst selection based on chemistry selection), while enabling the coupling of the decisions made at the process level with the resulting product properties.

Framework

Superstructure architecture

The design of an ethanol upgrading biorefinery can be described in terms of three levels of decisions:

1) Selection of the species undergoing a chemical reaction; ethanol as the initial substrate is in the list of such species, but the selected strategy may involve subsequent transformations of other species (e.g., ethylene, butanol) produced from the initial ethanol transformation.

2) Selection of the specific chemistries used for the transformation of the species selected at the first level; for example, if ethanol and ethylene were selected, then the chosen chemistries may be alcohol dehydration and oligomerization, respectively.

3) Selection of the specific processes used to realize the chemistries chosen in the second level; these processes are characterized by the catalyst, the separation train used to obtain the products of interest, and the specific process conditions used.

In this work, we have used two abstractions to systematically account for these decisions. First, we represent upgrading strategies as a sequence of conversion modules consisting of a catalytic conversion unit and its associated separation operations. Second, we introduce a hierarchical architecture to consider the three relevant decision levels simultaneously (Figure 1).

The superstructure has three levels: *Module (Figure 1(a))*, *Technology (Figure 1(b))*, and *Technology group (Figure 1(c))*. The module, which is the elemental building block of this approach, can be understood as a conversion process designed to transform one or more species into a set of products. The operation of a module is described using four elements: (1) an inlet mixer (light yellow square in the Fig 1(a)) that combines inlet streams containing chemical species consumed in the module; (2) a conversion unit (light blue rectangle in Figure 1(a)), characterized by a set of yield coefficients determining the amount of each species produced or consumed per mol of substrate in every reaction occurring in the module; (3) an outlet splitter (red square in Figure 1(a)), described by a set of separation factors establishing the fraction of each chemical species directed toward each of the module's products; and (4) an optional source element (blue diamond in Fig 1(a)), accounting for the supply of carrier gases or reactants not present in the feed stream. Each module has base capital and operating costs defined with respect to a reference incoming mass flow rate. Note that all the information associated with the performance of separation units and reactors is lumped in the yield coefficients and separation factors, and the economics of the process in the capital and operating cost parameters.

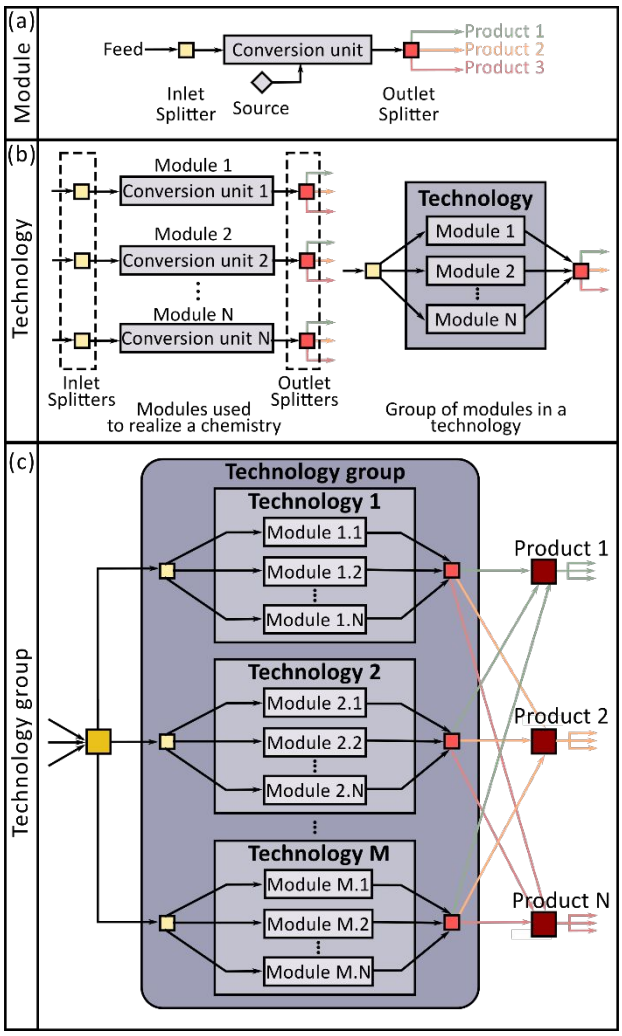

Figure 1. Elements of the superstructure (a) Module: processes used to accomplish the transformation of a substrate; (b) Technology: set of modules that can be used to realize a chemistry; (c) Technology group: set of technologies designed for the transformation a substrate. Note that the inlet and outlet splitters of the modules in a technology are merged (indicated as dashed squares); once the modules are merged into a technology, the labels for the elements (splitters, and conversion units) are dropped, and only the word "module" is used for simplicity.

Different modules can be synthesized for the realization of the same chemistry (e.g., ethanol dehydration can be accomplished using a process employing a SynDol® catalyst, or a process employing a zeolite catalyst). All the modules designed for the realization of the same chemistry are grouped in the second level of the superstructure termed as a *technology* (Figure 1(b)). Modules in a technology differ from each other either because they were designed using different catalysts or because they employ a different separation train. Only one module per technology can be selected. Thus, it is possible to lump together all the inlet mixers and outlet splitters associated with all the modules in a technology (Figure 1(b)), knowing that the only active streams (i.e. those with flow greater than zero) are those connected to the selected module. Finally, at the third level, all the technologies consuming the same substrate are grouped into a *technology group* (Figure 1(c)); for example, Guerbet coupling, condensation, and dehydration of ethanol belong to the same technology group because they process the same substrate. Since two technologies in the same technology group can be selected simultaneously, we do not constrain the system to prevent this kind of decision. In addition to the elements already described, a technology group contains an inlet splitter (dark yellow square in Figure 1(c)) and a set of outlet splitters (burgundy squares in Figure 1(c)). The inlet splitter distributes the incoming substrate stream toward the selected technologies. The output splitters distribute the obtained products toward the inlet splitters of other technology groups for further processing or toward the final products.

Optimization Model

The resulting optimization model, which couples process synthesis decisions and fuel properties, is a mixed integer non-linear program (MINLP) model (see SI1 for the details) that can be used to find the optimal process producing fuels with tailored properties [Eq. 1]. While, in general, various objective functions can be used (e.g., economic, environmental), in this paper we use profit maximization defined as the difference between revenues and costs. Two sources of revenue were considered: fuel and electricity sales, with the fuels selling price set at 2$US/kg based on a recent technoeconomic analysis (TEA)[68] and the electricity sold at 1.5×10^{-8} $US/J based on NREL report[8]. Costs have three components: annualized capital investment, operating costs, and feed stream costs (see supplementary S7 for details on feedstock cost). All costs and prices are in 2007 dollars to be consistent with the reference year of the most recent NREL work on lignocellulosic ethanol production[8].

$$\begin{aligned} &\max\ (\text{Profit [Eqs. S1} - \text{S6]}) \\ s.t.\ &\begin{cases} \text{Process model [Eqs. S7} - \text{S34]} \\ \text{Fuel model [Eqs. S35} - \text{S51]} \end{cases} \end{aligned} \tag{1}$$

The model is expressed using four types of sets: superstructure elements $i \in \mathbf{I}$ (subsets include: modules $\mathbf{I^{MD}}$, technologies $\mathbf{I^{TCH}}$, and technology groups $\mathbf{I^{TG}}$); chemical reactions $r \in \mathbf{R}$; chemical components $k \in \mathbf{K}$; and process streams $j \in \mathbf{J}$ (subsets include: fuel streams $\mathbf{J^P}$, and electricity streams $\mathbf{J^E}$). The process synthesis component of the model [Eqs. S7-S34] consists of mass balances written around the different elements of the superstructure, logical relations based on superstructure connectivity, capital costs scaling functions, and operating cost definitions. We introduce three binary variables accounting for the discrete decisions made at the different levels of the superstructure: module ($YM_i, i \in \mathbf{I^{MD}}$), technology ($YT_i$, $i \in \mathbf{I^{TCH}}$), and technology group ($YTG_i, i \in \mathbf{I^{TG}}$). Each of these binaries is equal to one if the respective module, technology, or technology group is selected. Additionally, we have one binary variable for each fuel product ($YF_j\ j \in \mathbf{J^P}$), with these binaries being equal to one if the corresponding fuel is produced. All the aforementioned binaries are used to inactivate process streams, introduce integer cuts to find alternative solutions, and define logical constraints based on the superstructure architecture (e.g. if a technology is not selected then the modules associated with that technology cannot be selected). The property model consists of two parts [Eqs. S35-S51]: blending rules for the calculation of target properties as a function of the fuel composition; and composition constraints limiting the amount of specific chemical species such that fuel standards are met (e.g., upper bounds on aromatic content). The process synthesis and fuel property models are coupled because the fuel composition is a function of the selected technology groups, technologies, and modules.

Ethanol upgrading

We employ the proposed framework to study ethanol upgrading. The available chemistries, catalysts, and processes are integrated to generate a superstructure (see Figure 2) with 14 technology groups and 25 technologies, incorporating process information for 87 different modules (See SI-2). We consider the possibility of using, exclusively or simultaneously, three different ethanol substrates with different water content: 50%, 7%, and 0% [Kg/Kg]. These concentrations were selected considering possible simplifications of the ethanol purification process. Specifically, a 50% blend can be obtained using only a beer distillation column; a 7% blend is close to the water ethanol azeotrope and can be obtained using a beer column followed by a rectification column; and a near 100% feedstock corresponds to the typical product of a bioethanol production plant in which both beer and rectification columns are used followed by a molecular sieving unit. Products include three fuel output streams: gasoline, jet fuel, and diesel; an electricity generation stream; and a waste stream. Although only energy products are considered in this work, the proposed framework can be readily extended to consider the co-production of other valuable chemicals[69,70]. All fuel streams are constrained such that the resulting products display a set of properties consistent with those of typically used fuels[71–73]. The considered properties as well as the enforced constraints are summarized in Table 1. Blending rules required for the estimation of these properties are described in the supplementary information (SI-1).

Table 1. Specifications for the fuel products considered in this study.

	Type	Gasoline	Jet Fuel	Diesel
RON	Min	91	-	-
CN	Min	-	-	40
Density [kg/m^3]	Max	775	840	845
Viscosity [mm^2/s]	Min	-	-	2.0
	Max	2.0	8	4.5
X_{30} **[%mol]**	Max	5	-	-
X_{215}**[%mol]**	Min	98	-	-
X_{160}**[%mol]**	Max	-	5	-
X_{300}**[%mol]**	Min	-	98.5	-
X_{150}**[%mol]**	Max	-	-	5
X_{360}**[%mol]**	Min	-	-	95
Olefins [%mol]	Max	18	2	20
Aromatics [%mol]	Max	35	25	35

RON: Research Octane Number. CN: Cetane Number
X_T: mol fraction of fuel evaporated at *T* temperature

Chemistries. Ethanol upgrading chemistries have been included based on recently published reviews[5,10] (See SI-5). At a high level, upgrading pathways can be described as a sequence of two main stages. In the first stage, ethanol is catalytically transformed into a set of products (Figure 1 Technology group 1); and in the second stage, which is not always required, the products of the first stage are converted into a final product that satisfies required specifications (Figure 1, Technology groups 2-14). We consider four chemistries for the initial ethanol transformation: dehydration[13,74,75], condensation[5,21,76–82], simultaneous dehydration and oligomerization[83–85], and Guerbet coupling[11,12,94,86–93]. The first two of these chemistries yield an olefin: ethylene in dehydration; and a catalyst-dependent blend of ethylene, propylene, and isobutene in condensation. In the case of simultaneous dehydration and oligomerization, the product is a mixture of olefins and aromatics suitable as a gasoline or jet fuel replacement. Finally, we have Guerbet coupling, an old chemistry that has captured renewed attention due to its ability to upgrade ethanol into higher alcohols with high selectivity. Most of the products obtained in the first stage can be clustered into two groups: olefins, and higher alcohols. Hence in the second stage we are interested in chemistries associated with these products.

In the case of olefins, the chemistries of interest are limited to oligomerization[9,16–19], for which several processes, involving heterogeneous and homogeneous catalysts, have been developed. Although oligomerization reactions yield a mixture of branched and linear olefins, we have assumed, due to limited information for the catalysts of interest, that we obtain mainly linear olefins. In the case of higher alcohols there are three chemistries of interest: dehydration[95–100], Guerbet coupling[86], and etherification[86,98,101,102]. The first two have already been discussed, but the difference here is that the products obtained when higher alcohols are used as substrates have a higher number of carbons. Etherification has been gaining attention because ethers of higher alcohols have very promising properties for tailor-made diesel fuel[86]. From a fuel design perspective, the wide range of chemistries available leads to a large feasible space for the design of advanced fuels. A detailed list of all the species considered and their relevant properties is presented in the supplementary information (See SI-4).

Catalysts. The design and characterization of catalysts available for the aforementioned chemistries has received considerable attention in the literature[5,10,12,15,16,19]. A survey of available catalyst for the chemistries of interest is presented in the supplementary information (See SI-5). Given the large number of available catalysts it is impractical to include all of them in the superstructure. Instead, we use a subset of carefully selected catalysts to represent a broad range of operating conditions and selectivities for each chemistry. The catalyst selection is based on a clustering procedure, in which we group together catalysts with similar selectivity under similar operating conditions. Next, from each cluster we select only one representative catalyst (see SI-2 and SI-5). This procedure reduces the size of the problem while still maintaining a diverse set of alternatives. For the clustering we consider five criteria with a strong bearing on process design: *operating temperature*, *operating pressure*, *single pass conversion*, *selectivity*, and *catalysis phase* (i.e. homogeneous or heterogeneous). We note that each catalyst incorporated in the superstructure can be used in one or more *modules* (See SI-2 for the list of catalyst used in each module, and SI-6 for process details), each of which has an associated set of reactions (See Table S2-1). We note that while most of the chemistries considered have been used in the petrochemical or the bio-renewables industries[3,5,13,16,83], many of the catalysts included in the framework have been tested only at a laboratory scale. However, the corresponding data are included in order to have a broader design space.

ARTICLE

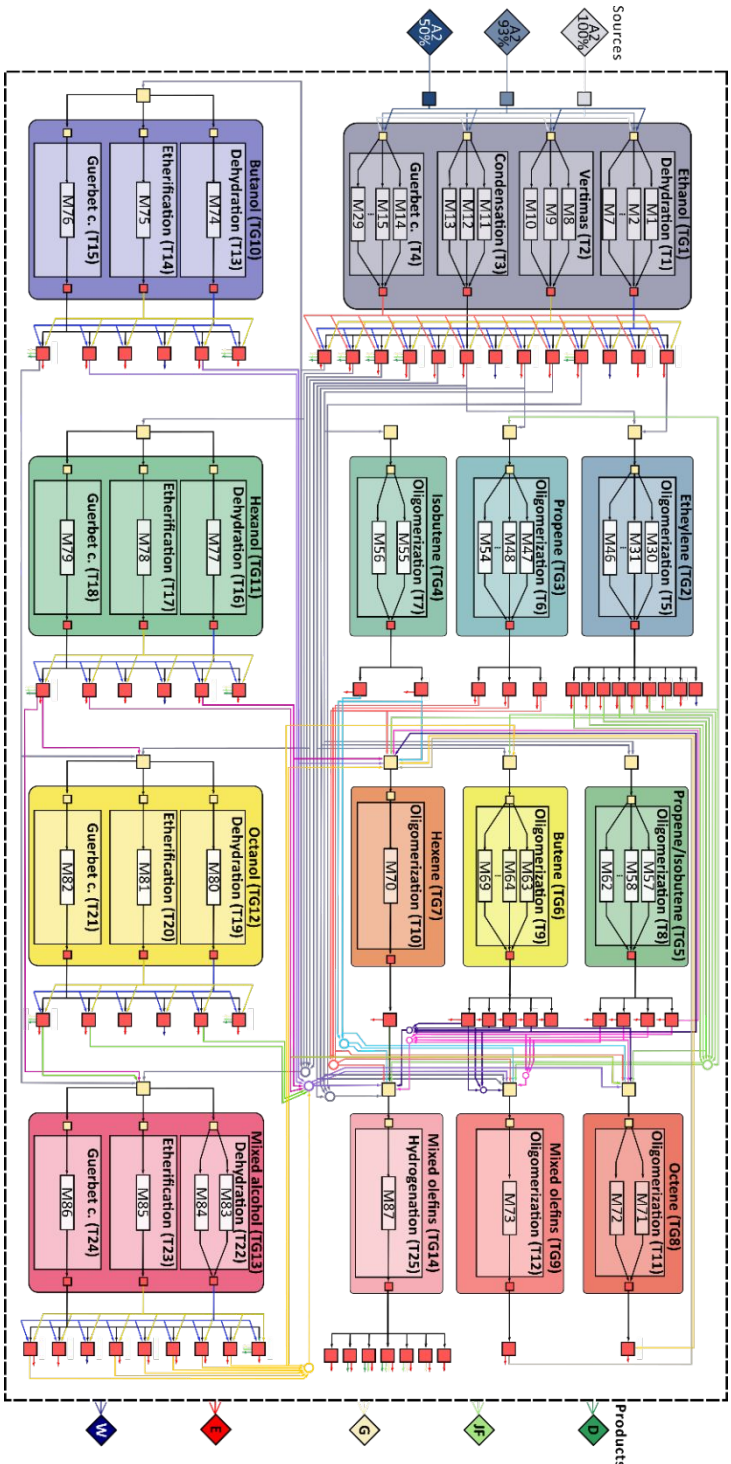

Figure 2. Ethanol upgrading superstructure illustrating the different technology groups (TG), technologies (T) and modules (M) used. Sources and final products are illustrated as diamonds to the left and right of the figure. Connections between technology groups are illustrated in accordance with the connectivity matrix in SI-3.

ARTICLE

Parameter calculation. There are 5 types of parameters used in the mathematical model that need to be estimated *a-priori*. Three types or parameters are process related: yield coefficients ($\eta_{r,k}$), separation factors ($\gamma_{j,j',k}$), and reference incoming mass flow rates ($\phi_i^{ref}\ i \in \mathbf{I^{MD}}$); and two economic: capital investment ($\phi_i^{CCM}\ i \in \mathbf{I^{MD}}$), and operating costs ($\phi_i^{OCM}\ i \in \mathbf{I^{MD}}$). To calculate the process parameters, we have mainly relied on dedicated process simulations performed in ASPEN plus V10® (files available upon request); and for the economic parameters we have prepared spreadsheets for the calculation of capital, and operating costs. A total of 85 different process flowsheets corresponding to the different modules were developed (See SI-6 for details). In each flowsheet energy integration was performed using Aspen Energy Analyzer, first by using a targeting approach to identify potential energy savings, and then by synthesizing a Heat Exchanger Network based on the identified targets. All financial assumptions used in these calculations are presented in SI-7. For a few processes (2 out of 87), we collected the required information from available technoeconomic analysis (TEA) studies, ensuring that the economic parameters were adjusted in accordance with the assumptions used in this work. Economic parameters ϕ_i^{CCM} and ϕ_i^{OCM}, and the reference mass flow rate ϕ_i^{ref} are summarized for each module in the supplementary information SI-8.

Solution of optimization models. The superstructure optimization problem was implemented in GAMS and solved using the global optimization solver BARON[103]. Solution times vary depending on the problem at hand, but for the results presented in this work they ranged between 1 and 12 hours.

Results

Optimal ethanol upgrading biorefineries

We are interested in finding optimal upgrading biorefineries for the transformation of ethanol into fuels with tailored properties. This question can be posed either generally, such that a multiproduct biorefinery is admissible; or in a more restricted way such that a single product biorefinery is pursued. In this last case, constraints on the admissible products are introduced using the binaries associated with each fuel ($YF_j \in j \in \mathbf{J^P}$). We study four cases: a multiproduct biorefinery (Figure 3), and three biorefineries in which a single fuel product with properties similar to those of gasoline (Figure 4), jet fuel (Figure 5), or diesel (Figure 6) is obtained. Panel A in Figures 3 through 6 show a Sankey diagram illustrating mass flow across the biorefineries. In this diagram technologies that are part of the biorefinery appear as green blocks and the catalysts selected are indicated in the text; the flow of different streams is illustrated using areas of different color. The products (colored boxes on the right of the diagram) always include a waste sink, and an electricity generation sink (labeled as burn); fuel products on the other hand are added as needed based on the optimal biorefineries obtained. The results presented are normalized to 100 Kg of feed allowing an easy interpretation of the results. Panel B of Figures 3-6 presents the costs of the different biorefineries for a plant able to process ~ 500Ton-EtOH/day. Specifically, it shows a bar plot with the major costs (annualized capital (CC), operating cost excluding feedstock (OC), and feedstock) and revenues (from fuel and electricity sales); we also show two bar plots detailing the capital and operating costs breakdown. Finally, panel C shows the fuel composition, and properties of each product. We note that our results have been obtained assuming constant fuel prices, which implies that market variations may lead to decreased economic benefit. In principle, the proposed approach can be extended to a stochastic programming setting, where first stage decisions yield the biorefinery design, and second stage decisions yield operational strategies in different scenarios. However, the resulting formulations would be computationally expensive and are beyond the scope of this paper. Nevertheless, we note that the proposed model can still be used to find strategies that allow mitigation of the impact of price variability in the case of multiproduct biorefineries. Specifically, flows can be reconfigured among the selected blocks to optimize an updated objective function. The interested reader can find the details of this approach in SI 10.

Multiproduct biorefinery. The obtained biorefinery consists of three processing modules: Guerbet coupling, followed by two modules connected in parallel for the processing of C6 alcohols: etherification and alcohol dehydration (Figure 3(a)). The biorefinery mainly produces a gasoline compatible blendstock with a yield of 70.4 Kg/Kg-Ethanol; however, there is also some minor production of a diesel compatible blendstock with a yield of 5.7 Kg/Kg-Ethanol. We see that the gasoline fuel product consists of a blend of oxygenates (alcohols, aldehydes, ketones and esters) of low carbon number (C4-C6) and C6 olefins, with the main component been butanol, an alcohol that has been identified in the literature as a candidate replacement for gasoline with significant advantages over ethanol[104] (Figure 3(c)). The blendstock obtained for diesel fuel is simpler and consists of a blend of alcohols with six carbons and its ethers (C12). In terms of fuel properties, we highlight that the diesel fraction produced just meets the ASTM cetane number requirement (i.e. $CN = 40$), while the gasoline fraction is high quality with a RON number above 95.

Gasoline biorefinery. The biorefinery obtained for the exclusive production of a gasoline blendstock (Figure 4(a)) is very similar to that in Figure 3(a), except for the absence of the etherification module. Which leads to a small reduction in the total fuel yield (from 76.1 Kg/Kg-feed to 75.7 Kg/Kg-feed), and the capital ($81 million instead of $82.6 million) and operating costs ($8.3 million instead of $9.0 million). While minor savings in costs do not compensate for the lost revenue from products, the reduction in profit is only marginal ($129.7 million instead of $130 million). This reduction in profit is compensated by a reduction in biorefinery complexity, and it may be considered advantageous. The product profile obtained (Figure 4(c)) consists mainly of butanol and C6 olefins, as in the previous case. The importance of the coupling between process and product modelling is clearly manifested in the results presented in Figure 4. A naïve approach to the process synthesis problem, disregarding the fuel properties, would assume that the alcohol blend leaving the Guerbet

module (mainly butanol and hexanol) can be used as a gasoline blendstock. Only by considering the properties of the final product it is possible to identify the need of an intermediate process (in this case a dehydration module) to adjust the properties of the final fuel blend to the required specifications.

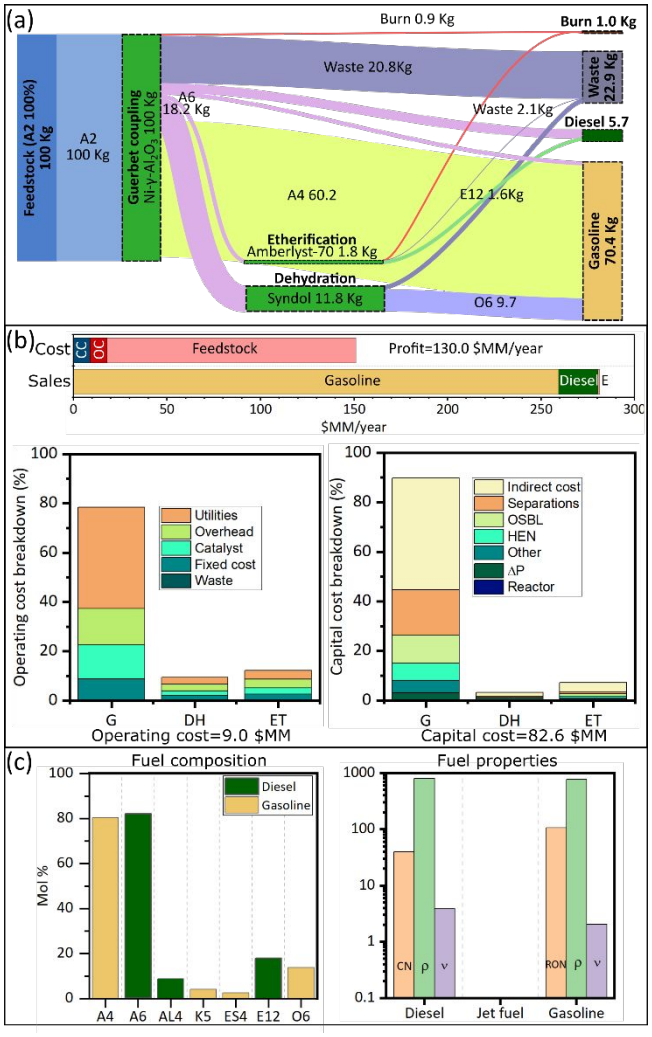

Figure 3. Optimal multiproduct biorefinery. (a) Sankey diagram based on mass flow. Technologies and modules selected are: Guerbet coupling (G), etherification (ET), and alcohol dehydration (DH). (b) Capital and operating costs breakdown. (c) Product composition and fuel properties (CN: for cetane number, ρ: density [kg/m^3], ν: viscosity [mm^2/s]). Chemical notation for carbon containing molecules consists of an alphabetic part indicating the functional group (A: alcohols, Al: aldehydes, K: ketones, Es: esters, O: olefins, E: ethers), and a numerical portion for the number carbons.

Middle distillates biorefineries. The biorefineries obtained for the production of middle distillates (Figures 5(c-Jet fuel) and 6(d-Diesel)) are similar consisting of a Guerbet coupling module, followed by dehydration and a set of oligomerizations that end in a hydrogenation module used for the transformation of olefins into paraffins. Diesel and jet fuel biorefineries differ in the oligomerization sequence, the specific modules selected, and the presence of an etherification module in the jet fuel biorefinery. Importantly, the higher degree of dehydration (note the presence of an alcohol dehydration module in Figures 3(c)-(d)) required in these biorefineries leads to a lower product yield (~60%), and therefore a lower profit: ~$66 million/year for the jet fuel biorefinery and ~$78 million/year for the diesel biorefinery, versus ~$130 million/year for the multiproduct and gasoline biorefineries. The reduction in profit is also influenced by the higher capital ($117.9 million (Jet fuel) and $89 million (diesel)) and operating costs ($16.9 million (Jet fuel) and $13.5 million (Diesel)) required in these biorefineries. The increase in costs in middle distillate biorefineries in comparison with the multiproduct (Figure 3) or gasoline (Figure 4) biorefineries is related to their higher complexity (7 modules). The jet fuel and diesel blends obtained consist of a mixture of oxygenates and olefins. In terms of fuel properties, in both cases a low viscosity blend is produced (0.002Pa-s (jet fuel) and 0.0025Pa-s (Diesel)); importantly, the diesel fuel obtained displays a cetane number of approximately 60, characteristic of a premium product.

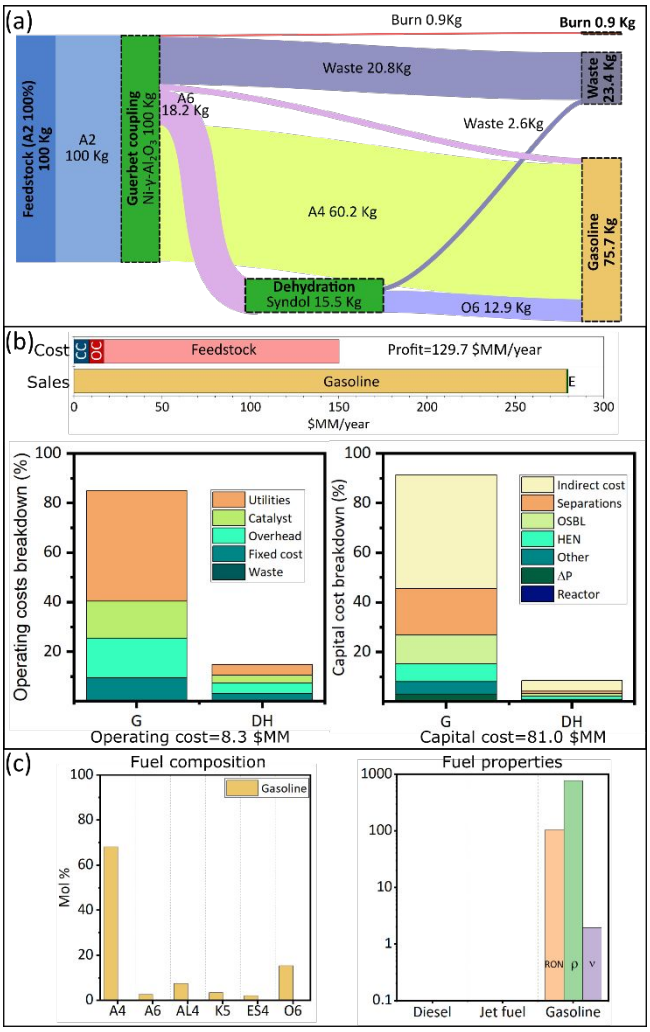

Figure 4. Optimal gasoline biorefinery. (a) Sankey diagram based on mass flow. Technologies and modules selected are: Guerbet coupling (G), and alcohol dehydration (DH). (b) Capital and operating costs breakdown. (c) Product composition and fuel properties (CN: for cetane number, ρ: density [kg/m^3], ν: viscosity [mm^2/s]). Chemical notation for carbon containing molecules consists of an alphabetic part indicating the functional group (A: alcohols, Al: aldehydes, K: ketones, Es: esters, O: olefins, E: ethers), and a numerical portion for the number carbons.

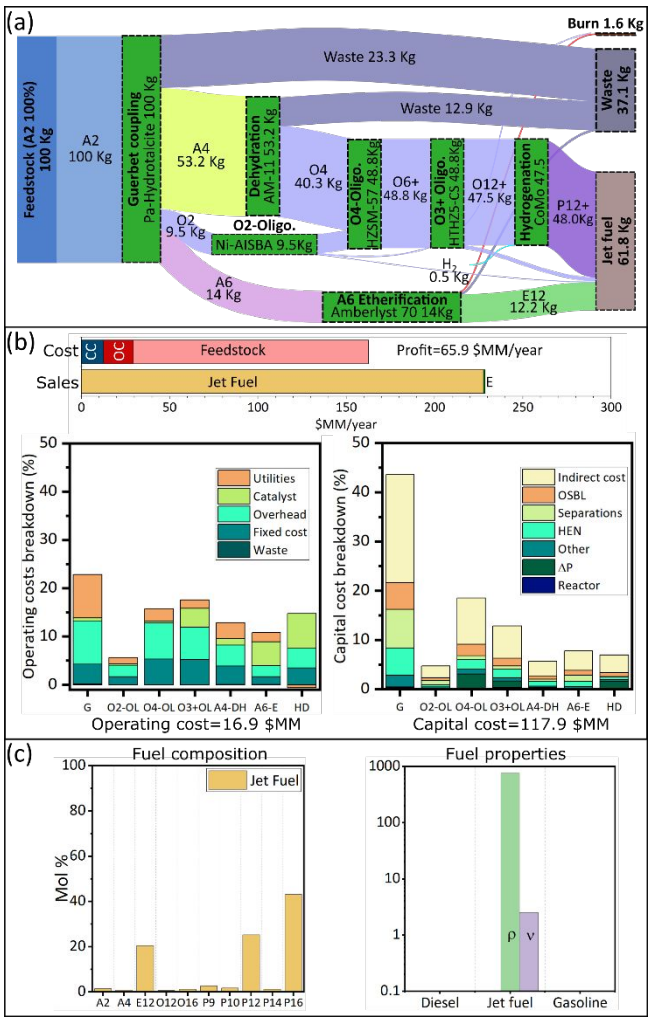

Figure 5. Optimal jet fuel biorefinery. (a) Sankey diagram based on mass flow. Technologies and modules selected are: Guerbet coupling (G), butanol dehydration (A4-DH), ethylene oligomerization (O2-OL), butene oligomerization (O4OL), olefins (C3+) oligomerization (O3+OL), hydrogenation (HD), and hexanol etherification (A6-E). (b) Capital and operating costs breakdown. (c) Product composition and fuel properties (CN: for cetane number, ρ: density [kg/m^3], v: viscosity [mm^2/s]). Chemical notation for carbon containing molecules consists of one alphabetic portion indicating the functional group (A: alcohols, E: ethers, O: olefins, P: paraffins), and a numerical portion for the number carbons.

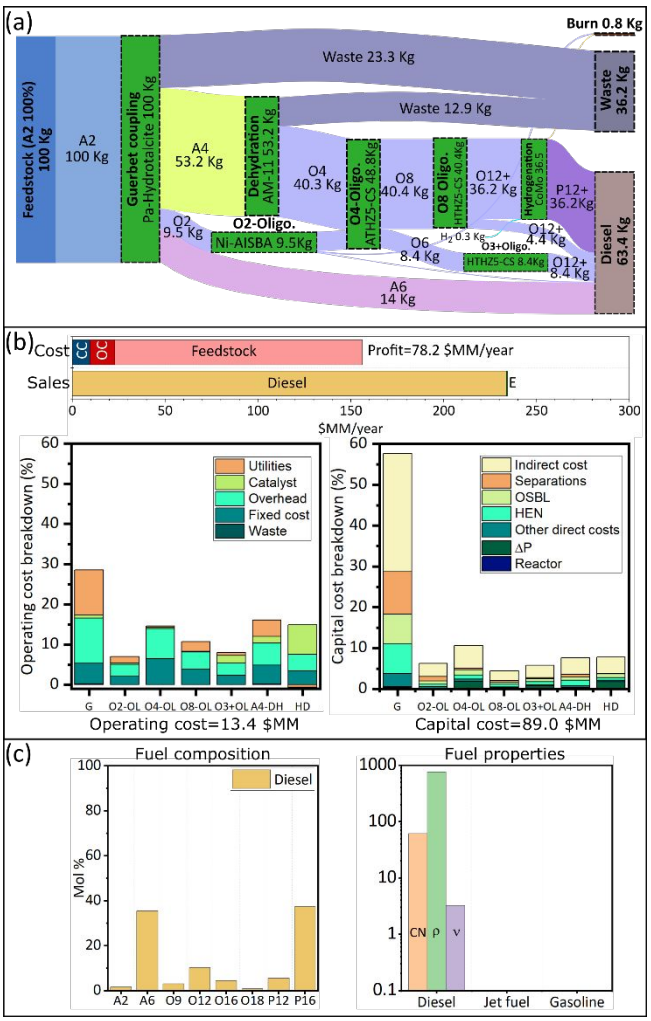

Figure 6. Optimal diesel biorefinery. (a) Sankey diagram based on mass flow. Technologies and modules selected are: Guerbet coupling (G), Ethylene oligomerization (O2-OL), Butene oligomerization (O4-OL), Butanol dehydration (A4-DH), octene oligomerization (O8-OL), olefins (C3+) oligomerization (O3+OL), and olefins hydrogenation (HD). (b) Capital and operating costs breakdown. (c) Product composition and fuel properties (CN: for cetane number, ρ: density [kg/m^3], v: viscosity [mm^2/s]). Chemical notation for carbon containing molecules consists of an alphabetic portion indicating the functional group (A: alcohols, O: olefins, P: paraffins), and a numerical portion for the number carbons.

Discussion

The results obtained stress the significance of the framework adopted, not only we were able to select an optimal biorefinery in economic terms, but also the process was tailored such that specific products with predefined properties were obtained. The fuel mixtures produced by the optimal biorefineries cannot be designed by intuition nor by applying heuristics. Only the use of process and systems engineering simultaneously considering process and fuel property constraints has enabled the design of biorefineries for the production of advanced fuels.

Some insights can be obtained by analyzing the cost distribution of the processes studied. In all biorefineries the dominant cost driver is feedstock (bar plot in Figures 3(b)-6(b)). Capital and operating costs (other than feedstock) account together for less than 20% of the annualized production cost. Specifically, the total capital investment is on the order of $100 million (annualized to $10 million/year for a 30 years project) in all cases; while the operating costs are between $10-$20 million/year. In contrast, the feedstock cost is close to ~$130 million/year. From a process engineering perspective this implies that biorefineries in which a higher yield is obtained are favored if the goal is to maximize the profit. Consequently, in all the optimal biorefineries Guerbet chemistry is selected. This chemistry is the one with the higher mass yield among the options for ethanol upgrading (Technology group 1). The reason for this higher yield is that Guerbet chemistry leads only to a partial dehydration. Conversely, other chemistries available for the initial ethanol transformation, like

condensation and dehydration, fully dehydrate alcohols and therefore lead to a lower yield. In the case of condensation, the mass loss is even greater due to the loss of carbon in the form of carbon oxides.

The results suggest that there are two research directions that may lead to improvements in the economics of biofuel production. First, since the total product yield is so impactful on the economics, it is critical to develop highly selective catalysts, leading to less waste products, or by-products that cannot be incorporated in the final fuel. Second, in the case of Guerbet chemistry, the catalysts developed so far require the use of anhydrous ethanol. Thus, potential savings may be obtained if water tolerant catalyst are developed. Ethanol with a higher content of water is cheaper, especially when the concentration is below the azeotrope. Some advances have been reported in this direction[87]. Also, improved efficiency in water-ethanol separation could have a positive effect. Although capital and operating costs (excluding feedstock) are not as impactful as the feedstock cost, improvements on these variables may lead to better economics. Finally, we see that the Guerbet coupling module, the largest one, dominates capital (43%-91%) and operating (23%-78%) costs (Figures 3(b)-6(b)). Thus, pointing to the need of developing compact and efficient Guerbet coupling modules to improve the economics of the designed biorefineries.

Process complexity vs. efficiency

An important point regarding the biorefineries obtained for middle distillates (Figures 5 and 6) is that their complexity, measured by the number of modules, is high (7 modules each), which may hinder its practical application. Thus, it is of interest to understand the effect of constraining the maximum number of modules. This consideration can be easily studied by introducing an additional constraint into the proposed optimization model. Specifically, if one is interested in obtaining biorefineries displaying a maximum number of modules it is sufficient to specify that $\sum_{i \in \mathbf{I}^{MD}} YM_i < a$, where "$a$" is an integer number. For the case of a diesel biorefinery, the results obtained when a reduced number of modules is used are presented in Figures 7 and 8. It can be seen that constraining the maximum number of modules leads to simpler biorefineries (Figure 7) at the expense of reducing the profit. The Pareto front showing the trade-off between profit and complexity (number of modules) is shown in Figure 8(a). Note, for example, that the profit obtained when 7 modules are used is ~$78 million/year, whereas when three modules are used this value decreases more than 50% to ~$30 million/year. This reduction in profit is explained by a reduction in the fuel product yield. For the biorefinery in Figure 6(a) (7 modules) the yield is ~63%, in contrast for the biorefinery in Figure 7(b) (4 modules) the yield is ~51%. Changes in the biorefinery configuration caused by constraining the maximum number of modules lead to changes in the final product composition and its properties (Figure 8 (b)-(c)). The most evident change is the increase in alcohols in the final product as the maximum number of modules decreases, this change leads to products with lower cetane number. Which is expected provided that alcohols have lower cetane numbers than olefins with the same number of carbons.

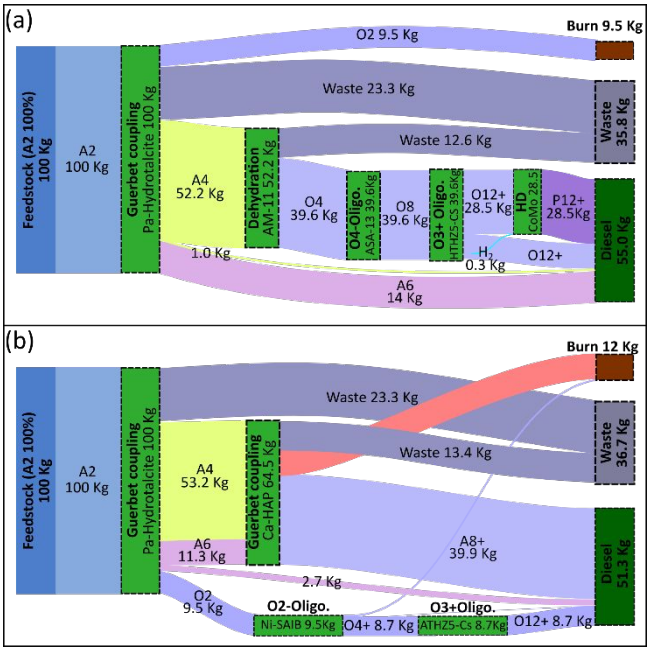

Figure 7. Sankey diagram based on mass flow for diesel production biorefineries when the number of modules is constrained to be less or equal than 5 (a) and less or equal than 4 (b).

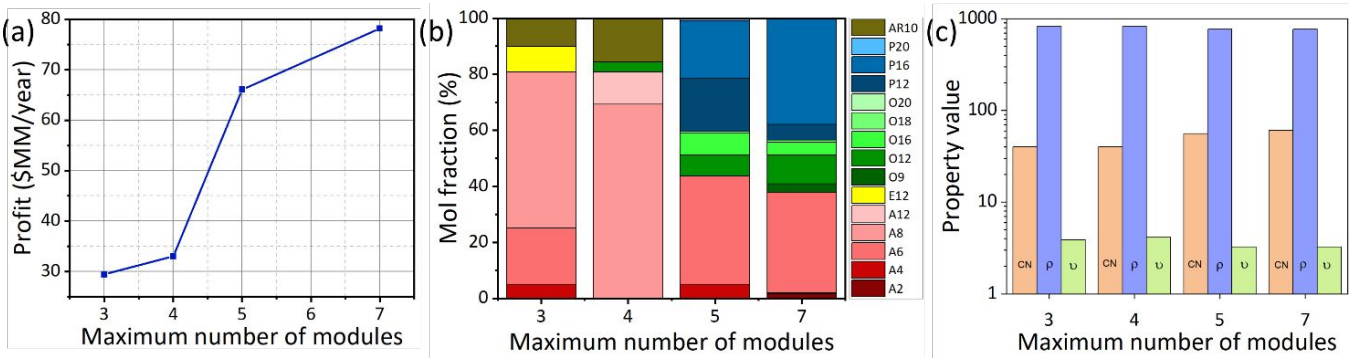

Figure 8. (a) Pareto front showing the trade-off between profit and maximum number of modules. (b) Diesel fuel composition (alcohols are shown in red shades, ethers in yellow, olefins in green, paraffins in blue, and aromatics in brown). (c) Properties or products from biorefineries with different number modules. Fuel properties (CN: for cetane number, ρ: density [kg/m^3], v: viscosity [mm^2/s]). Chemical notation for carbon containing molecules consists of an alphabetic portion indicating the functional group (A: alcohols, E: ethers, O: olefins, P: Paraffins, Ar: aromatics), and a numerical portion for the number carbons.

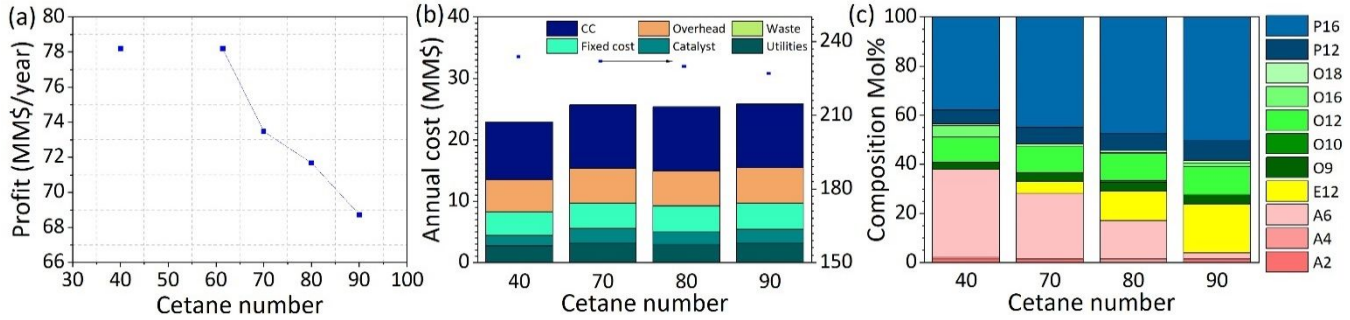

Figure 9. Effects of changing the cetane number (CN) constraint on the optimal processes selected for a diesel biorefinery. (a) Pareto front. (b) Breakdown of processing cost for each biorefinery. (c) Composition of diesel products obtained. Chemical notation for carbon containing molecules consists of an alphabetic portion indicating the functional group (A: alcohols, E: ethers, O: olefins, P: paraffins), and a numerical portion for the number carbon

Understanding the trade-off between fuel properties and profit

The trade-off between fuel properties and profit can be studied by tightening the constraints on the fuel property model. We study the impact of tightening the cetane number requirements in a diesel biorefinery (Figure 9 and Figure SI.9). As shown in Figure 9(a), the profit starts to decrease as a function of cetane number once the product specification constraint becomes binding. For example, when the required cetane number increases from 61.4 (value at which the constraint becomes binding) to 80 the profit is reduced by approximately 8% ($6 million/year). Changes in costs and sales as a function of cetane number can be seen in Figure 9(b), where we present a detailed breakdown of the cost components for the optimal biorefineries obtained for different cetane number specifications. Requiring a higher cetane number results in a smaller feasible space in terms of processes, that is, there are fewer configurations able to yield a product with the required properties. Details on the optimal processes obtained as a function of cetane number are presented in Supplementary Figure S9.1. Constraining the product has a direct impact on the selected processes. Changing the product requirements causes changes in the set of technologies selected (Figure S9.1); *e.g.* increasing the cetane number above 61.4 leads to biorefineries in which an etherification module is used. The size of the etherification module increases concomitantly with the cetane number requirement.

In addition to modifying the set of technologies selected, specification-related constraints also affect the modules selected to realize each technology. As an illustration, when we enforce $CN \geq 40$ or $CN \geq 70$, the module selected for the ethylene oligomerization process uses Ni-AISBA as catalyst. In contrast, when we enforce $CN \geq 80$ a Ni-LASA catalyst is selected. Both changes in the selected technologies and modules are aimed at modifying the final fuel product composition (Figure 9(c)) such that the property constraints are satisfied. For example, we see in Figure 9(c) that the amount of ethers, known for having a high cetane number, increases in the final product when higher cetane numbers are required. Likewise, the fraction of alcohols (A2, A4, and A6), all with cetane numbers lower than 20, decreases progressively as the specification on cetane number increases. This example clearly illustrates the interplay that exists between processes, fuel properties, and overall profit. Understanding and exploiting this relation is key for the design of biorefineries yielding tailored fuel products.

Identification of optimal strategy including a specific technology

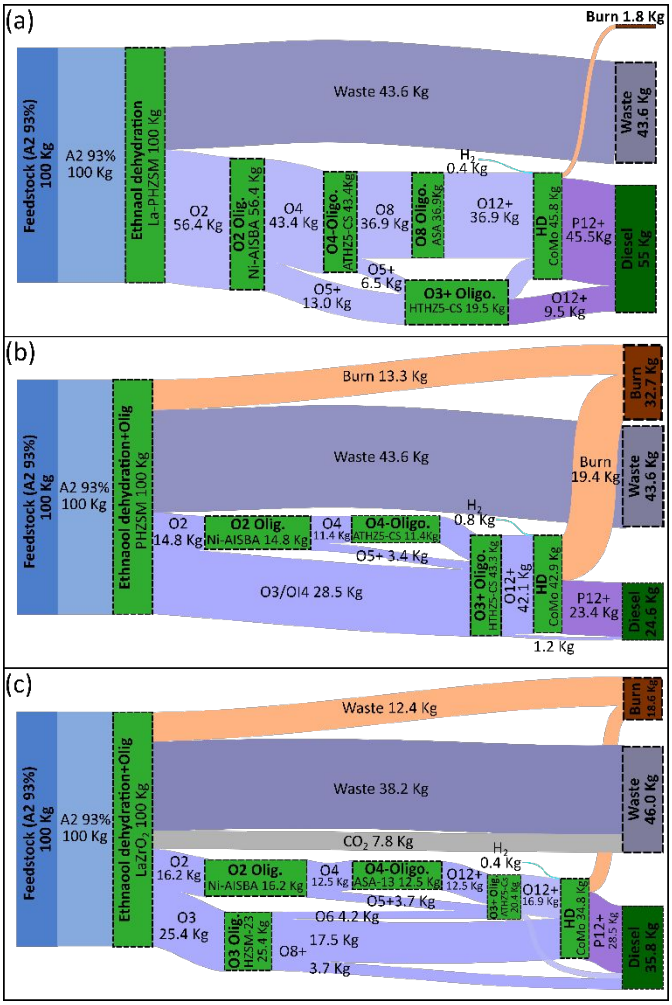

Figure 10. Sankey diagram based on mass flow for optimal biorefineries for diesel production such that ethanol is first catalytically transformed using dehydration to ethylene (a); simultaneous dehydration and oligomerization (b); and condensation (c).

One relevant question that often arises, both at the experimental and process design levels, is how to identify the optimal biorefinery for the production of a candidate biofuel that includes a particular technology or catalyst. The framework that we have developed is

suitable to address this kind of question. We investigate the design of biorefineries for the production of diesel fuel, employing the four technologies we consider for the initial ethanol transformation (*i.e.* dehydration, simultaneous dehydration and oligomerization, condensation, and Guerbet coupling). In addition to fixing the corresponding binary variables, we also enforce an additional condition preventing the system from selecting more than one technology in the first technology group ($\sum_i YT_i = 1, i \in \mathbf{I}_i^{\mathbf{T}}, \boldsymbol{i}' \in TG1$), thereby enforcing the use of the technology of interest to process all incoming ethanol flow.

The optimal biorefineries employing the first three technologies (*i.e.* dehydration, simultaneous dehydration and oligomerization, and condensation) are presented in Figure 10; results for the biorefinery that employs Guerbet coupling were already presented in Figure 6. With respect to the results shown in Figure 10, we observe that the strategies found involve the initial chemical transformation of ethanol followed by a set of oligomerization modules yielding a higher molecular weight product. Since the content of olefins is constrained in diesel fuels (see Table 1), the use of a hydrogenation module for the conversion of olefins into paraffins is required. In comparison with the diesel biorefinery using Guerbet coupling (Figure 6), the results in Figure 10 show an increase of almost 20% in the amount of waste water produced due to the higher degree of dehydration and the use of a substrate with higher water content (93% ethanol Kg/Kg). Another difference is the increase in the size of the stream used for electricity generation, especially in the strategies in Figure 10(b)-(c). This increase is caused by the generation of olefins that cannot be blended in the final product because their incorporation would cause an undesirable change in fuel properties.

Sensitivity analysis

Once an optimal biorefinery has been identified it can be further analyzed using sensitivity analysis tools to find the major cost drivers. In Figure 11, we show the effect of perturbing relevant cost parameters on the annualized production cost of the four diesel biorefineries presented (Figure 6 and Figure 10). Since the major driver in all systems is the feedstock cost, and it is already known, we have excluded it from the analysis to visualize and identify other cost drivers. We consider three cost parameters for each of the technologies employed: utilities (±20%), catalyst and other feedstocks (-50%/+100%), and total investment (+100% and -20%). Perturbation values have been selected to reflect likely scenarios. In the case of utilities, changes of ±20% are considered due to better heat integration (-20%) or the need of incorporating additional separation units. Catalyst and other feedstocks costs on the other hand may change significantly because these are novel processes; for example, the cost of a catalyst can be reduced either by increasing its activity or by improving its manufacturing process. Finally, changes in the total investment reflect the risk associated with the installation of a first-of-a-kind system (+100%); and the less likely possibility of obtaining a better design (-20%) with similar functionality. In all cases three alternatives to achieve improvements in the process economics are identified. First, the cost of utilities is significant, especially for the ethanol processing technology, therefore optimizing heat integration is critical. Second, the consumption of catalyst and hydrogen in the hydrogenation module has a significant economic burden, therefore it is relevant to find alternatives to use by-product hydrogen as a feedstock. Finally, reducing the total investment cost associated with the ethanol processing technology (*i.e.* dehydration, dehydration and oligomerization, condensation or Guerbet coupling) plays an important role. The ethanol processing technology handles the largest amount of mass, consequently it is the most capital intensive.

Conclusions

In this paper, we have systematically studied the upgrading of ethanol toward advanced fuels with tailored properties. To integrate catalysis, process synthesis and fuel property modelling, we developed a superstructure-based optimization framework that simultaneously considers product (fuel) and process design. Using this framework, we explored the synthesis of biorefineries for the production of gasoline, diesel, and jet fuel. Additionally, we study the trade-off between process complexity and profit, and the relation between fuel specifications and process synthesis. Finally, we show how the framework developed can be used for the identification of the optimal biorefinery associated with a particular technology or catalyst. The results show the interdependencies between the specifications of the fuels and the processes used to obtain those fuels. Either changing the target fuels or their specifications leads to biorefineries in which different technologies are selected. Likewise, the chemical composition of the products changes as a function of the fuel property constraints. Understanding and exploiting these interdependencies is fundamental in the development of processes for fuels with superior properties. These results suggest that to unlock the full potential of a bio-based economy, systematic approaches, allowing us to design efficient processes for non-intuitive high-performance fuel blends, are necessary.

ARTICLE

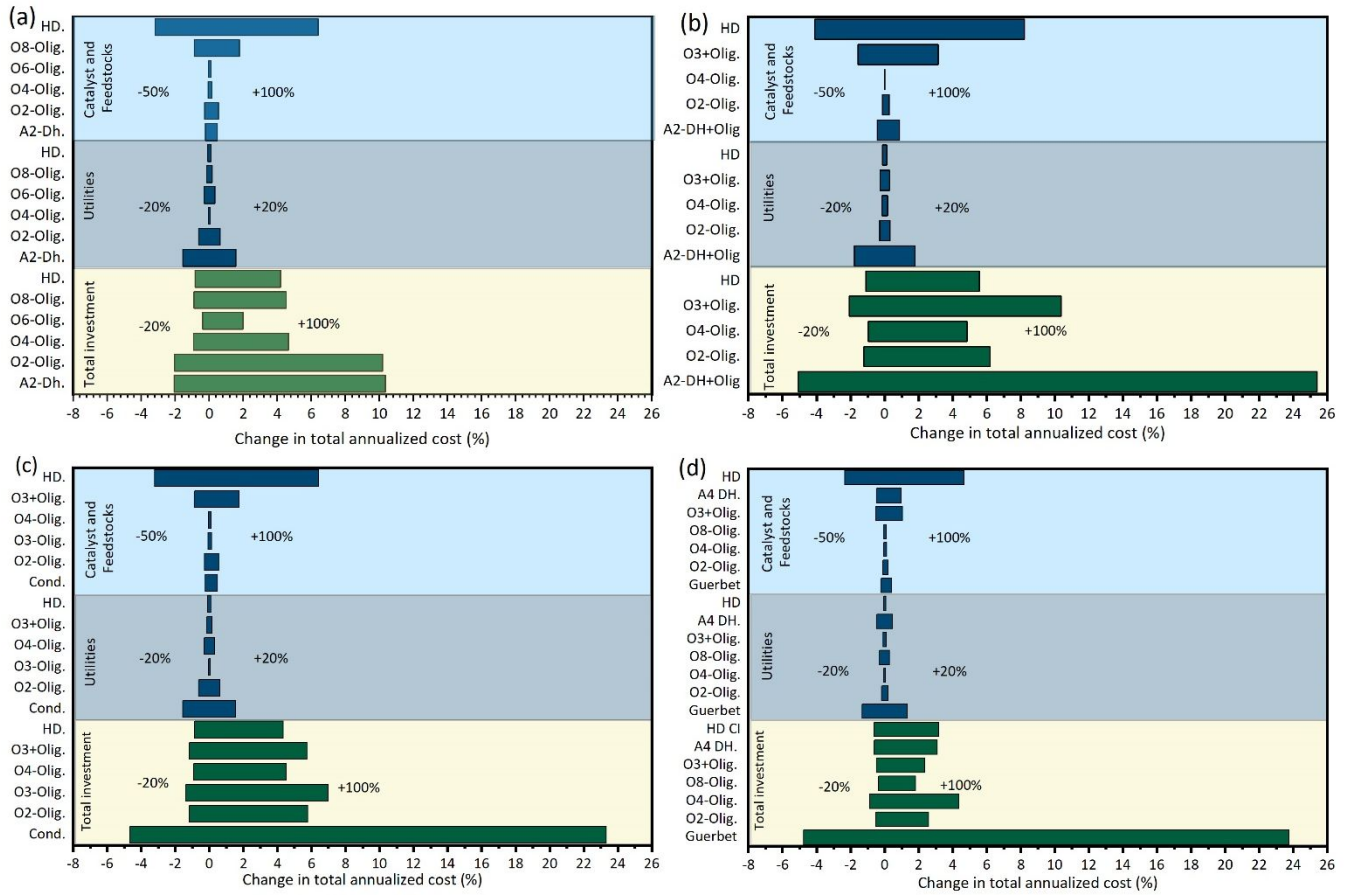

Figure 11. Tornado plot showing changes in the annualized production cost (excluding feedstock) when different cost parameters are perturbed: utilities (±20%), catalyst and other feedstocks (-50%, +100%), and total investment (-20%, +100%).(a) Diesel biorefinery based on ethanol Guerbet coupling (See Figure 6). (b) Diesel biorefinery based on ethanol dehydration (See Figure 10(a)). (c) Diesel biorefinery based on ethanol dehydration plus oligomerization (See Figure 10(b)) (d) Diesel biorefinery based on ethanol condensation (See Figure 10(c)). Blue squares are show operating costs while green squares show the capital investment. The y-axis shows the modules used, labelled using three identifiers: (i) an alphabetic component indicating the functional group of the substrate (A: alcohols, O: olefins); (ii) a numerical character indicating the number carbons of the substrate; and (iii) an alphabetic contraction indicating the chemistry used (DH: dehydration, Olig: oligomerization, HD: hydrogenation, Cond: condensation).

Conflicts of interest

There are no conflicts to declare.

Acknowledgements

This work was funded by the U.S. Department of Energy, grant number DE-EE0008480.

References

[1] EIA, (n.d.).
[2] P. Fasahati and C.T. Maravelias, Joule **2**, 1915 (2018).
[3] L. Tao, J.N. Markham, Z. Haq, and M.J. Biddy, Green Chem. **19**, 1082 (2017).
[4] U.S. Energy Information Agency, *Annual Energy Outlook 2019 with Projections to 2050* (2019).
[5] N.M. Eagan, M.D. Kumbhalkar, J.S. Buchanan, J.A. Dumesic, and G.W. Huber, Nat. Rev. Chem. **3**, 223 (2019).
[6] International Energy Agency, *The Future of Trucks: Implications for Energy and the Environment* (2017).
[7] M. Slupska and D. Bushong, Biofuels, Bioprod. Biorefining **13**, 857 (2019).
[8] D. Humbird, R. Davis, L. Tao, C. Kinchin, D. Hsu, A. Aden, P. Schoen, J. Lukas, B. Olthof, M. Worley, D. Sexton, and D. Dudgeon, *Process Design and Economics for Biochemical Conversion of Lignocellulosic Biomass to Ethanol: Dilute-Acid Pretreatment and Enzymatic Hydrolysis of Corn Stover* (Golden, Colorado, 2011).
[9] V. Zacharopoulou and A.A. Lemonidou, Catalysts **8**, (2018).
[10] J. Sun and Y. Wang, ACS Catal. **4**, 1078 (2014).
[11] H. Aitchison, R.L. Wingad, and D.F. Wass, ACS Catal. **6**, 7125

(2016).
[12] J.T. Kozlowski and R.J. Davis, ACS Catal. **3**, 1588 (2013).
[13] D. Fan, D.J. Dai, and H.S. Wu, Materials (Basel). **6**, 101 (2013).
[14] J.A. Posada, A.D. Patel, A. Roes, K. Blok, A.P.C. Faaij, and M.K. Patel, Bioresour. Technol. **135**, 490 (2013).
[15] A. Finiels, F. Fajula, and V. Hulea, Catal. Sci. Technol. **4**, 2412 (2014).
[16] A. V. Lavrenov, T.R. Karpova, E.A. Buluchevskii, and E.N. Bogdanets, Catal. Ind. **8**, 316 (2016).
[17] V. Hulea, ACS Catal. **8**, 3263 (2018).
[18] C.P. Nicholas, Appl. Catal. A Gen. **543**, 82 (2017).
[19] B.M. Antunes, A.E. Rodrigues, Z. Lin, I. Portugal, and C.M. Silva, Fuel Process. Technol. **138**, 86 (2015).
[20] A. Galadima and O. Muraza, Ind. Eng. Chem. Res. **54**, 7181 (2015).
[21] J. Saavedra Lopez, R.A. Dagle, V.L. Dagle, C. Smith, and K.O. Albrecht, Catal. Sci. Technol. **9**, 1117 (2019).
[22] A.R.R. Ciric and C.A. Floudas, Comput. Chem. Eng. **14**, 241 (1990).
[23] C.A. Floudas, A.R. Ciric, and I.E. Grossmann, AIChE J. **32**, 276 (1986).
[24] J. Ryu and C.T. Maravelias, AIChE J. (2020).
[25] H. Yeomans and I.E. Grossmann, Ind. Eng. Chem. Res. **39**, 1637 (2000).
[26] H. Yeomans and I.E. Grossmann, Comput. Chem. Eng. **23**, 709 (1999).
[27] L. Kong and C.T. Maravelias, Ind. Eng. Chem. Res. **57**, 6330 (2018).
[28] W. Wu, C.A. Henao, and C.T. Maravelias, AIChE J. **62**, 3199 (2016).
[29] C.A. Henao and C.T. Maravelias, AIChE J. **57**, 1296 (2011).
[30] E.A. del Rio-Chanona, D. Zhang, and N. Shah, AIChE J. **64**, 91 (2018).
[31] J. Kim, S.M. Sen, and C.T. Maravelias, Energy Environ. Sci. **6**, 1093 (2013).
[32] P.E. Murillo-Alvarado, J.M. Ponce-Ortega, M. Serna-González, A.J. Castro-Montoya, and M.M. El-Halwagi, Ind. Eng. Chem. Res. **52**, 5177 (2013).
[33] A. Kelloway and P. Daoutidis, Ind. Eng. Chem. Res. **53**, 5261 (2014).
[34] J. Gong and F. You, Ind. Eng. Chem. Res. **53**, 1563 (2014).
[35] J. Gong and F. You, AIChE J. **64**, 123 (2018).
[36] B. Bao, D.K.S. Ng, D.H.S. Tay, A. Jiménez-Gutiérrez, and M.M. El-Halwagi, Comput. Chem. Eng. **35**, 1374 (2011).
[37] E. Zondervan, M. Nawaz, A.B. de Haan, J.M. Woodley, and R. Gani, Comput. Chem. Eng. **35**, 1752 (2011).
[38] D.H.S. Tay, D.K.S. Ng, N.E. Sammons, and M.R. Eden, Ind. Eng. Chem. Res. **50**, 1652 (2011).
[39] L.Y. Ng, V. Andiappan, N.G. Chemmangattuvalappil, and D.K.S. Ng, Comput. Chem. Eng. **81**, 288 (2015).
[40] D.H.S. Tay, D.K.S. Ng, H. Kheireddine, and M.M. El-Halwagi, Clean Technol. Environ. Policy **13**, 567 (2011).
[41] D. Schack, L. Rihko-Struckmann, and K. Sundmacher, Ind. Eng. Chem. Res. **57**, 9889 (2018).
[42] P. Cheali, J.A. Posada, K. V. Gernaey, and G. Sin, Biomass and Bioenergy **75**, 282 (2015).
[43] A.C. Kokossis, M. Tsakalova, and K. Pyrgakis, Comput. Chem. Eng. **81**, 40 (2014).
[44] D.K.S. Ng, Chem. Eng. Trans. **21**, 421 (2010).
[45] R.T.L. Ng, S. Patchin, W. Wu, N. Seth, and C.T. Maravelias, Biofuels Bioprod. Biorefining **12**, 170 (2018).
[46] A.D. Celebi, A.V. Ensinas, S. Sharma, and F. Maréchal, Energy **137**, 908 (2017).
[47] V. Pham and M.M. El-Halwagi, AICHE J. **58**, 1212 (2012).
[48] M.O. Bertran, R. Frauzem, A.S. Sanchez-Arcilla, L. Zhang, J.M. Woodley, and R. Gani, Comput. Chem. Eng. **106**, 892 (2017).
[49] M. Dahmen and W. Marquardt, Energy and Fuels **31**, 4096 (2017).
[50] F.T. Eljack, M.R. Eden, V. Kazantzi, X. Qin, and M.M. El-Halwagi, AIChE J. **53**, 1232 (2007).
[51] A. König, L. Neidhardt, J. Viell, A. Mitsos, and M. Dahmen, Comput. Chem. Eng. **134**, (2020).
[52] W.A. Marvin, S. Rangarajan, and P. Daoutidis, Energy and Fuels **27**, 3585 (2013).
[53] V. Kazantzi, X. Qin, M. El-Halwagi, F. Eljack, and M. Eden, Ind. Eng. Chem. Res. **46**, 3400 (2007).
[54] M. Hechinger, A. Voll, and W. Marquardt, Comput. Chem. Eng. **34**, 1909 (2010).
[55] M. Dahmen, M. Hechinger, J. Victoria Villeda, and W. Marquardt, SAE Int. J. Fuels Lubr. **5**, 990 (2012).
[56] R. Gani, Comput. Chem. Eng. **28**, 2441 (2004).
[57] E. Conte and R. Gani, AIChE J. **57**, 2431 (2011).
[58] H. Hashim, M. Narayanasamy, N.A. Yunus, L.J. Shiun, Z.A. Muis, and W.S. Ho, J. Clean. Prod. **146**, 208 (2017).
[59] A. Voll and W. Marquardt, AIChE J. **58**, 1788 (2012).
[60] K. Ulonska, M. Skiborowski, A. Mitsos, and J. Viell, AIChE J. **62**, 3096 (2016).
[61] S. Rangarajan, A. Bhan, and P. Daoutidis, Appl. Catal. B Environ. **145**, 149 (2014).
[62] P. Daoutidis, W.A. Marvin, S. Rangarajan, and A.I. Torres, AIChE J. **59**, 215 (2012).
[63] X. Zhou, Z.J. Brentzel, G.A. Kraus, P.L. Keeling, J.A. Dumesic, B.H. Shanks, and L.J. Broadbelt, ACS Sustain. Chem. Eng. **7**, 2414 (2019).
[64] B.H. Shanks and P.L. Keeling, Green Chem. **19**, 3177 (2017).
[65] M.B. Viswanathan, D.R. Raman, K.A. Rosentrater, and B.H. Shanks, Processes **8**, (2020).
[66] S. Maronese, A. V. Ensinas, A. Mian, A. Lazzaretto, and F. Maréchal, Ind. Eng. Chem. Res. **54**, 7038 (2015).
[67] A. Quaglia, B. Sarup, G. Sin, and R. Gani, Comput. Chem. Eng. **38**, 213 (2012).
[68] W.-C. Wang, L. Tao, J. Markham, Y. Zhang, E. Tan, L. Batan, M. Biddy, W.-C. Wang, L. Tao, Y. Zhang, E. Tan, E. Warner, and M. Biddy, *Review of Biojet Fuel Conversion Technologies-NREL/TP-5100-66291* (2016).
[69] K. Huang, P. Fasahati, and C.T. Maravelias, IScience **23**, 100751 (2020).
[70] R.T.L. Ng, P. Fasahati, K. Huang, and C.T. Maravelias, Appl. Energy **241**, 491 (2019).
[71] J. Bacha, J. Freel, A. Gibbs, L. Gibbs, G. Hemighaus, K. Hoekman, J. Horn, M. Ingham, L. Jossens, D. Kohler, D. Lesnini, J. McGeehan, M. Nikanjam, E. Olsen, R. Organ, B. Scott, M. Sztenderowicz, A. Tiedemann, C. Walker, J. Lind, J. Jones, D. Scott, and J. Mills, Chevron Glob. Mark. 1 (2007).
[72] ASTM D4814−14b, *Standard Specification for Automotive Spark-Ignition Engine Fuel* (2014).
[73] ASTM D1655-19a, *Standard Specification for Aviation Turbine Fuels* (2010).
[74] A. Mohsenzadeh, A. Zamani, and M.J. Taherzadeh, ChemBioEng Rev. **4**, 75 (2017).
[75] M. Zhang and Y. Yu, Ind. Eng. Chem. Res. **52**, 9505 (2013).
[76] F. Xue, C. Miao, Y. Yue, W. Hua, and Z. Gao, Fuel Process. Technol. **186**, 110 (2019).
[77] F. Wang, W. Xia, X. Mu, K. Chen, H. Si, and Z. Li, Appl. Surf. Sci. **439**, 405 (2018).
[78] F. Hayashi and M. Iwamoto, ACS Catal. **3**, 14 (2013).
[79] W. Xia, F. Wang, L. Wang, J. Wang, and K. Chen, Catal. Letters (2019).
[80] W. Xia, X. Mu, F. Wang, K. Chen, H. Si, and Z. Li, React. Kinet. Mech. Catal. **122**, 473 (2017).

[81] M. Iwamoto, Catal. Today **242**, 243 (2015).
[82] F. Liu, Y. Men, J. Wang, X. Huang, Y. Wang, and W. An, ChemCatChem **9**, 1758 (2017).
[83] J.R. Hannon, L.R. Lynd, O. Andrade, P.T. Benavides, G.T. Beckham, M.J. Biddy, N. Brown, M.F. Chagas, B.H. Davison, T. Foust, T.L. Junqueira, M.S. Laser, Z. Li, T. Richard, L. Tao, G.A. Tuskan, M. Wang, J. Woods, and C.E. Wyman, Proc. Natl. Acad. Sci. 201821684 (2019).
[84] Z. Song, A. Takahashi, I. Nakamura, and T. Fujitani, Appl. Catal. A Gen. **384**, 201 (2010).
[85] W. Xia, K. Chen, A. Takahashi, X. Li, X. Mu, C. Han, L. Liu, I. Nakamura, and T. Fujitani, Catal. Commun. **73**, 27 (2016).
[86] N.M. Eagan, B.J. Moore, D.J. McClelland, A.M. Wittrig, E. Canales, M.P. Lanci, and G.W. Huber, Green Chem. (2019).
[87] I. Nezam, L. Peereboom, and D.J. Miller, J. Clean. Prod. **209**, 1365 (2019).
[88] J. Pang, M. Zheng, L. He, L. Li, X. Pan, A. Wang, X. Wang, and T. Zhang, J. Catal. **344**, 184 (2016).
[89] C. Zhang, K. Balliet, and victor J. Johnston, US 8,962,897 B2 (2012).
[90] C. Zhang, K. Balliet, and V.J. Johnston, US 9,024,090 B2 (2012).
[91] E.C. Tan, L.J. Snowden-Swan, M.T. Abhijit-Dutta, S. Jones, K.K. Ramasamy, M. Gray, R. Dagle, A. Padmaperuama, Ma. Gerber, A.H. Sahir, L. Tao, and Y. Zhang, Biofuels, Bioprod. Biorefining **11**, 41 (2016).
[92] C. Zhang, US 2014/0179958 A1 (2012).
[93] C. Zhang, M. Borlik, and H. Weiner, WO2014100131A1 (2014).
[94] H.S. Ghaziaskar and C.C. Xu, RSC Adv. **3**, 4271 (2013).
[95] P. Brandão, A. Philippou, J. Rocha, and M.W. Anderson, Catal. Letters **80**, 99 (2002).
[96] Y.S. Hsu, Y.L. Wang, and A.N. Ko, J. Chinese Chem. Soc. **56**, 314 (2009).
[97] N.P. Makgoba, T.M. Sakuneka, J.G. Koortzen, C. Van Schalkwyk, J.M. Botha, and C.P. Nicolaides, Appl. Catal. A Gen. **297**, 145 (2006).
[98] R.J.J. Nel and A. De Klerk, Ind. Eng. Chem. Res. **48**, 5230 (2009).
[99] T.T.N. Nguyen, V. Ruaux, L. Massin, C. Lorentz, P. Afanasiev, F. Maugé, V. Bellière-Baca, P. Rey, and J.M.M. Millet, Appl. Catal. B Environ. **166–167**, 432 (2015).
[100] M.E. Wright, US20120238788A1 (2012).
[101] C. Casas, R. Bringué, E. Ramírez, M. Iborra, and J. Tejero, Appl. Catal. A Gen. **396**, 129 (2011).
[102] E. Medina, R. Bringué, J. Tejero, M. Iborra, and C. Fité, Appl. Catal. A Gen. **374**, 41 (2010).
[103] N. V. Sahinidis, J. Glob. Optim. **8**, 201 (1996).
[104] D. Gschwend, P. Soltic, A. Wokaun, and F. Vogel, Energy and Fuels **33**, 2186 (2019).